

# Effect of Different Types of Filler and Filler Loadings on the Properties of Carboxylated Acrylonitrile–Butadiene Rubber Latex Films

Z. N. Ain, A. R. Azura

*School of Materials and Mineral Resources Engineering, Universiti Sains Malaysia, 14300 Nibong Tebal, Pulau Pinang, Malaysia*

Received 13 July 2009; accepted 6 June 2010

DOI 10.1002/app.32984

Published online 21 September 2010 in Wiley Online Library (wileyonlinelibrary.com).

**ABSTRACT:** The effects of different types of fillers and filler loadings on the properties of carboxylated nitrile rubber (XNBR) latex were identified. Silica, mica, carbon black (CB; N330), and calcium carbonate ( $\text{CaCO}_3$ ) were used as fillers with filler loadings of 10, 15, and 20 parts per hundred rubber. Furnace ashing and Fourier transform infrared analysis proved that interaction existed between the fillers and XNBR latex films. The morphology of the filled XNBR films was significantly different for different types of fillers. Mica and  $\text{CaCO}_3$  fillers showed uneven distribution within the XNBR film, whereas other fillers, such as silica and CB, showed homogeneous distribution within the films. In the observation, silica and mica fillers also illustrated some degree of agglomeration. The mechanical

properties (e.g., tensile and tear strengths) showed different trends with different types of fillers used. For silica and mica fillers, the mechanical properties increased with filler loadings up to a certain loading, and decreased with higher filler loadings. For CB filler, the mechanical properties increased gradually with increasing filler loadings.  $\text{CaCO}_3$  fillers did not increase the mechanical properties. The crosslinking density of the XNBR films increased when they were incorporated with fillers because of the presence of elastomer–filler and filler–filler interactions. © 2010 Wiley Periodicals, Inc. *J Appl Polym Sci* 119: 2815–2823, 2011

**Key words:** crosslinking; FTIR; fillers; mechanical properties

## INTRODUCTION

Latex materials have been the subject of recent extensive research and development. As a result, their application areas have been expanding. Natural rubber latex products have good physical and chemical properties. However, the discovery that natural protein stabilizers can cause allergic reactions has limited their use. These chemicals result in dermal allergic responses, usually in the form of skin rashes and eczema. They can affect people who work in the medical field and who use latex gloves for protection.<sup>1</sup> The medical field has, thus, begun to steer clear of the use of natural rubber products in surgery and has instead leaned toward the use of synthetic rubbers to avoid allergy problems. Because of this, new latex raw materials, such as a styrene–butadiene rubber or a carboxyl-group-containing ionomer-based elastomer such as carboxylated nitrile rubber (XNBR), have been used.

Synthetic elastomers are typically not self-reinforcing elastomers. For example, nitrile elastomers do

not crystallize when they are stretched, and they require reinforcing fillers to develop their optimum tensile strength and tear resistance. In the latter instance, the fillers are intentionally added to the polymer systems. Fillers not only reduce the cost of the material but also improve the mechanical and dynamic properties of the compounds. In the rubber industry, carbon black (CB) and silica are the most widely used fillers.<sup>2</sup> CB imparts strength and toughness to elastomers; this improves rubber's resistance to tear, abrasion, and flex fatigue and increases its traction and durability. Normally, as the filler content increases, a moderate decrease in tensile strength and stiffness takes place together with improvements in the thermomechanical properties.<sup>3–6</sup>

Fillers are normally added to latex compounds to either stiffen the products, to reduce the cost, or to color the products. The presence of significant levels of filler particles in latex compounds will also affect the flow behavior. This is because the overall volume fraction of the disperse phase in the compound is altered (usually increased) and partly because the colloidal equilibrium may be disturbed; thereby, structures are allowed to develop between the dispersed particles.<sup>7</sup>

To this date, there have been no suitable fillers reported for carboxylated acrylonitrile–butadiene (XNBR) latex. This study was, therefore, carried out

Correspondence to: A. R. Azura (azura@eng.usm.my).

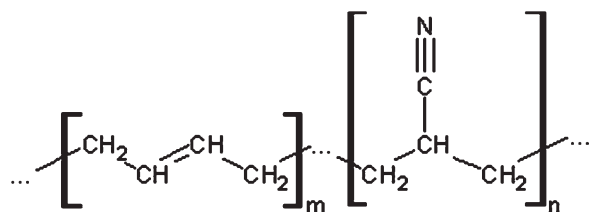


Figure 1 Chemical structures of XNBR.<sup>8</sup>

to investigate the effects of different types of fillers and filler loadings on the properties of XNBR latex films. The fillers used were silica, mica, calcium carbonate ( $\text{CaCO}_3$ ), and CB. These fillers were chosen because they are commonly used fillers in elastomer materials. The morphology of the fracture surfaces were observed through scanning electron microscopy (SEM), and the modification of chemical bonding was investigated with Fourier transform infrared (FTIR) spectroscopy. All tests were carried out according to the standard test methods for latex/rubber materials.

## EXPERIMENTAL

### Materials and ingredients

The XNBR latex used in this study was Perbunan N Latex VT-LA, which was supplied by Polymer Latex (Selangor, Malaysia). The chemical structure of XNBR is shown in Figure 1.<sup>8</sup> Other ingredients [sulfur, zinc oxide, potassium hydroxide, zinc diethyldithiocarbamate (ZDEC), and antioxidant] were supplied by Farben Technique (M) Sdn. Bhd. (Sendirian Berhad, Penang, Malaysia). The fillers used in this study were supplied by Sterling Chemicals, India (silanated silica and unsilanated mica), Nikko Kogyo Co. (Tokyo, Japan) ( $\text{CaCO}_3$ ), and Cabot Co. (M) Sdn. Bhd., Kuala Lumpur, Malaysia (CB type N330). The compounding ingredients and amounts used for this study are presented in Table I.

### Compounding and film preparation

We prepared the XNBR latex compounds by compounding all of the ingredients shown in Table I. All fillers in the form of powder were converted to dispersions by ball milling in a porcelain container for 48 h to reduce the particle size to the colloidal range (normally below 5  $\mu\text{m}$ ). The pH of the dispersions was adjusted to make it similar to that of the XNBR latex. All ingredients were added to the XNBR latex and stirred at 250 rpm for 0.5 h at room temperature. The compound was then matured for 48 h before it was used to make the dipped films.

Thin articles can be produced through dipping, but a coagulant is usually used to produce thicker

XNBR latex films. The coagulant was a 10% aqueous calcium nitrate solution, which was applied to the former by a dipping process and then dried at 80°C for about 5 min. The coagulant-treated film was dipped into the XNBR latex compound with a dwell time of 10 s to ensure a uniform thickness and then dried at 80°C for 10 min. The latex film was then dried at room temperature until it cooled before the stripping process.

### Chemical analysis

#### Furnace ashing

The filler weight percentage was determined through the ashing technique, which consisted of the elimination of the organic component of the composite by heating at a constant temperature. Each of the XNBR specimens weighed about 1 g and was placed into an ignited, weighed porcelain crucible. The specimens were then ashed in a muffle furnace at  $550 \pm 25^\circ\text{C}$  for 1 h. The porcelain crucibles were removed from the furnace, cooled in desiccators, and weighed. The weight percentage of the filler fraction in the materials was considered to be the difference in the weight before ashing ( $W_0$ ) and the weight immediately after ashing ( $W_1$ ), according to the following equation:

$$\text{Filler (wt\%)} = \frac{W_1}{W_0} \times 100$$

#### FTIR spectroscopy measurements

Infrared spectroscopic analysis of various XNBR latex films were carried out with a PerkinElmer Spectrum One spectrometer (Massachusetts, USA) with wave numbers ranging from 550 to 4000  $\text{cm}^{-1}$ . The FTIR operating parameters for this study are reported in Table II.

### Physical and mechanical properties tests

#### SEM analysis

The fracture surfaces of the XNBR latex films were investigated with a Zeiss Supra 35VP scanning

TABLE I  
Formulations for the XNBR Latex Compounding

Ingredient	Parts by weight	
	Dry	Wet
45.0% VT-LA	100.0	222.2
53.4% ZDEC	0.2	0.4
10.0% potassium hydroxide	1.0	10.0
33.0% zinc oxide	10.0	30.3
50.0% antioxidant	0.5	1.0
32.0% filler <sup>a</sup>	10, 15, 20	70, 105, 140

<sup>a</sup> Colloidal silica, mica,  $\text{CaCO}_3$ , or CB.

**TABLE II**  
**FTIR Operating Conditions**

FTIR parameter	Setting
Wavelength scanning range	4000–550 cm <sup>-1</sup>
Resolution	4 cm <sup>-1</sup>
Scan interval	1 cm <sup>-1</sup>
Number of scans	4

electron microscope (Oberkochen, Germany). The fractured ends of the specimens were mounted on aluminum stubs and sputter-coated with a thin layer of gold to prevent electrostatic charging during examination.

#### Tensile and tear tests

To investigate the tensile properties of rubber materials, an Instron IX3366 universal tensile tester (Norwood, USA) was used. For this purpose, the sample materials were cut from the dipped XNBR latex films into a dumbbell shape. The samples were placed in the sample holder, and their length, width, and thickness were measured. The test was done according to ASTM D 412-92 at a 500 mm/min crosshead speed.

*Tear strength* is defined as the force per unit thickness required to caused a nick out in test samples when it they are stretched under a constant rate in a direction perpendicular to the plane of sample preparation. Tear tests were performed with the Instron IX3366 universal testing machine according to ASTM D 624 with crescent test pieces type C at a 500 mm/min crosshead speed. For both tests, five samples were used, and the average results are reported.

#### Crosslinking density measurements

The crosslinking densities of the XNBR latex films were measured through a swelling method with toluene as the solvent. The XNBR latex films were weighed and allowed to swell in an excess of toluene for 48 h at 40°C. The swollen samples were taken after the equilibrium swelling period, blotted with filter paper, and weighed quickly in a weighing bottle. The samples were dried in an oven for 24 h at 70°C and weighed again. The volume fractions of the XNBR latex films in the swollen films ( $V_r$ ) were calculated with the following equation:

$$V_r = \frac{\left(\frac{m_1}{\rho_r}\right) - V_f}{\left(\frac{m_1}{\rho_r}\right) - V_f + \left(\frac{m_2 - m_3}{\rho_s}\right)}$$

where  $m_1$  is the initial weight of the specimen,  $m_2$  is the weight of the swollen specimen,  $m_3$  is the weight of the specimen after equilibrium,  $V_f$  is the volume of the filler,  $\rho_r$  is the density of rubber, and  $\rho_s$  is the density of the solvent (0.8669 for toluene). The cured

film crosslinking densities ( $n'$ s), the number of active network chain segments per unit volume, were determined through equilibrium swelling with the well-known Flory–Rehner equation;<sup>9</sup>  $V_r$  was substituted in the Flory–Rehner equation as follows:

$$n = -\frac{\ln(1 - V_r) + V_r + \mu V_r^2}{V_o \left[ (V_r)^{1/3} - \frac{V_r}{2} \right]}$$

where  $\mu$  is the parameter characteristic of interaction between the rubber network and the swelling agent and  $V_o$  is the molar volume of toluene ( $\mu = 0.39$ ).

## RESULTS AND DISCUSSION

### Determination of the filler content in the XNBR latex films by furnace ashing

The interactions between the fillers and rubbers will have a significant effect on the reinforcement properties of a filled elastomer.<sup>10</sup> The chemical and physical properties of the XNBR latex and filler and the amount of each present in a compound will influence these interactions. The values of the unfilled and filled XNBR latex films before and after ashing are presented in Table III. During ashing, most of the ZnO and other additive fillers were vaporized. Because a certain amount of ash was produced from the thermal decomposition of the unfilled XNBR latex film, it was necessary to first quantify this amount to subtract it from the total ash percentage produced from the filled sample and, thereby, obtain the filler contribution. This unfilled XNBR ash was quantified as 2.78% after the XNBR was ashed in a muffle furnace at 550 ± 25°C for 1 h. The results from Table III show that all filler values agreed with the actual filler loading used during compounding.

**TABLE III**  
**Values of the Unfilled and Filled XNBR Latex Films Before and After Ashing**

Filler content	Weight of the sample before ashing (g)	Weight of the sample after ashing (g)	Ash (%)	Filler (%)
Control	1.08	0.03	2.78	
10-phr silica	1.05	0.14	13.33	10.56
15-phr silica	1.06	0.19	17.92	15.15
20-phr silica	1.08	0.26	24.07	21.30
10-phr mica	1.05	0.14	13.33	10.56
15-phr mica	1.09	0.20	18.35	15.57
20-phr mica	1.05	0.25	23.81	21.03
10-phr CB	1.03	0.14	13.59	10.81
15-phr CB	1.03	0.19	18.45	15.67
20-phr CB	1.01	0.24	23.76	21.98
10-phr CaCO <sub>3</sub>	1.08	0.14	12.96	10.18
15-phr CaCO <sub>3</sub>	1.06	0.19	17.92	15.55
20-phr CaCO <sub>3</sub>	1.06	0.26	24.53	21.75

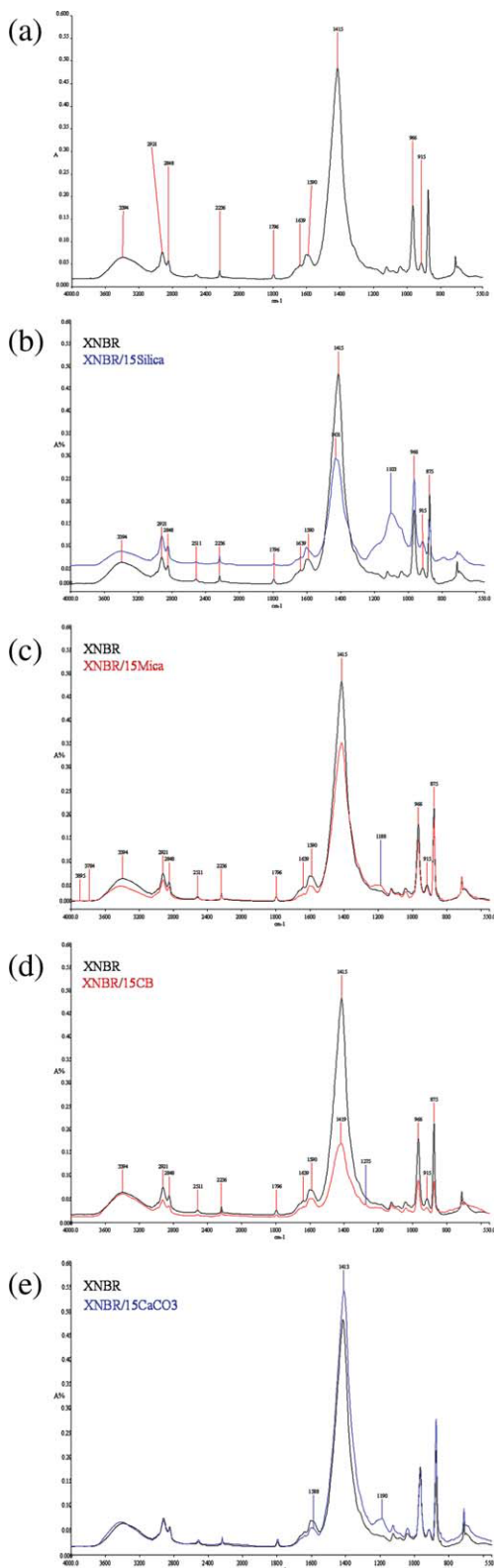


**Figure 2** FTIR spectrum of (a) unfilled XNBR, (b) XNBR/15silica, (c) XNBR/15mica, (d) XNBR/15 CB (e) XNBR/15  $\text{CaCO}_3$ . [Color figure can be viewed in the online issue, which is available at [wileyonlinelibrary.com](http://wileyonlinelibrary.com).]

### Characterization of the unfilled and filled XNBR latex films by FTIR analysis

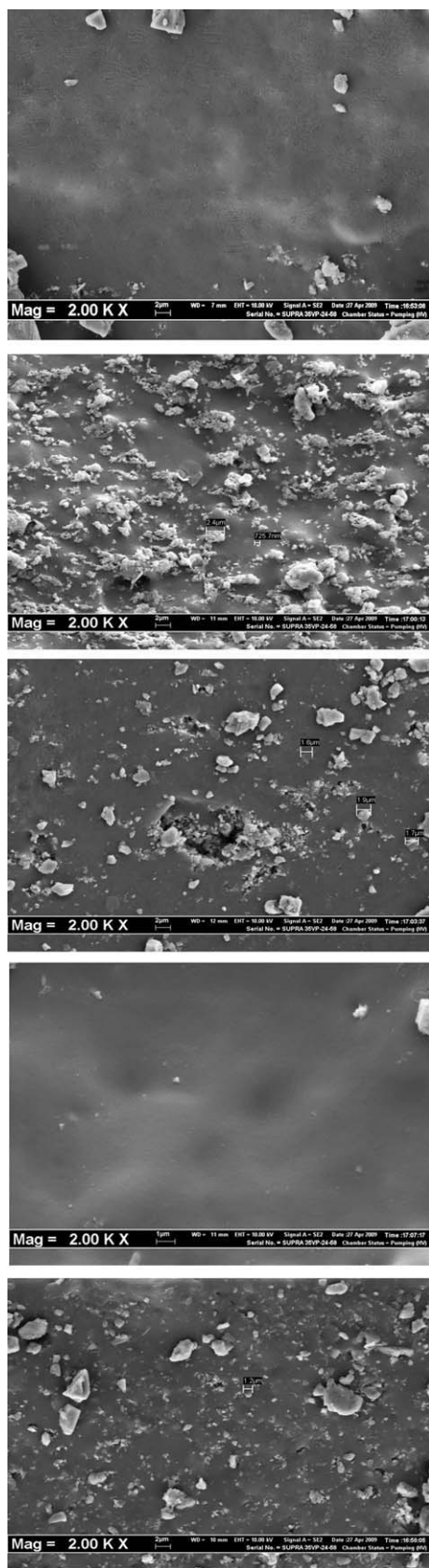
The nature of the chemical environments for the matrix–filler interaction groups within the films were probed with FTIR spectroscopy. In this study, 15 parts per hundred rubber (phr) filler loadings were chosen from each type of filler to investigate the effect of different types of fillers on the physical and mechanical properties of the XNBR latex films.

Figure 2(a) shows the FTIR spectra of the unfilled XNBR latex films, and Table IV shows the characteristic group frequencies for the unfilled XNBR film. The neat XNBR showed peaks in the range 1600–1800  $\text{cm}^{-1}$  due to the carboxylic part, which was responsible for the effects of C=O in different chemical environments. A bond at about 1590  $\text{cm}^{-1}$  was assigned to the asymmetric carbonyl stretching vibration of zinc carboxylate salt<sup>11</sup>; 2236  $\text{cm}^{-1}$  was the peak due to a triple bond of nitrile.<sup>12</sup> The other designated peaks at 915, 966, 1415, 1639, 2848, and 2921  $\text{cm}^{-1}$  were due to the hydrocarbon parts of the XNBR elastomer backbone.<sup>13,14</sup> The O–H stretching frequency of the acid dimer appeared as a broad band centered at about 3394  $\text{cm}^{-1}$ .

The analysis of the spectra of the XNBR film in Figure 2(b) showed that there was a very pronounced band appearing at 1103  $\text{cm}^{-1}$  after incorporation of the XNBR latex with silica. This band corresponded to the vibration absorption of the silane group (Si–O–C) present in the elastomer network, which normally exists within the ranges 800–850 and 1100–1200  $\text{cm}^{-1}$ .<sup>15</sup> The existence of this group proved the interactions of silica with the rubber chains. Figure 2(c) shows a broad band centered at about 1188  $\text{cm}^{-1}$ ; this band confirmed the existence of the silane group (Si–O–C) in the compound. As shown in this spectrum, very inadequate functional groups were detected in the XNBR latex filled with mica filler; this suggested very limited chemical

**TABLE IV**  
Characteristic Group Frequencies of the Unfilled XNBR Film

Wave number ( $\text{cm}^{-1}$ )	Assignment
915	Out-of-plane vibration of the methylene hydrogen atom of the vinyl group
966	Out-of-plane vibration of the hydrogen atom of the 1,4-trans component
1415	In-plane deformation of the methylene group
1590	Stretching of zinc carboxylate salt
1639–1670	Stretching of C=C
1796	Carbonyl stretching of monocarboxylic acid
2236	Stretching of nitrile triple bonds
2848	Symmetric stretching of the methylene group
2921	Asymmetric stretching of the methylene group
3394	O–H stretching of the acid dimer



**Figure 3** Morphologies of (a) unfilled XNBR film (b) XNBR/15silica, (c) XNBR/15mica, (d) XNBR/15CB, (e) XNBR/15CaCO<sub>3</sub>, at 2000 $\times$  magnification.

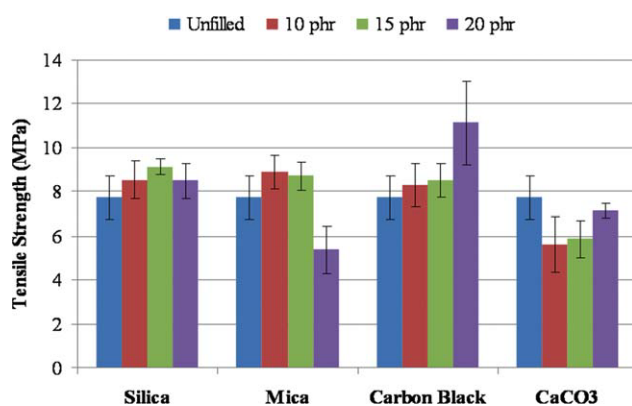
interaction between the XNBR latex and the mica filler. This result corresponded to the poor mechanical properties of the XNBR/mica latex films, which are discussed later.

Figure 2(d) shows a very weak band at 1275  $\text{cm}^{-1}$ , which represents the existence of the C—O—C stretching of vinyl ether. The intensity of absorbance was decreased in the band at 1415  $\text{cm}^{-1}$ , which corresponded to the C—O stretching of the dimers. These spectra showed that the chemical bonding in the raw XNBR latex films was altered, and CB successfully produced contact between the XNBR latex. The FTIR spectrum shown in Figure 2(e) showed that the intensity of absorbance decreased at 1588  $\text{cm}^{-1}$  and increased at 1415  $\text{cm}^{-1}$ . These bands corresponded to the asymmetric carbonyl stretching of calcium carboxylate and the C—O stretching of the dimers, respectively.<sup>14</sup> This showed that CaCO<sub>3</sub> produced a chemical interaction with the XNBR latex. Furthermore, the appearance of a new band at 1190  $\text{cm}^{-1}$  proved the chemical interaction between XNBR and the CaCO<sub>3</sub> filler at 15-phr loading. This band was assigned to the C—O—C stretching of the ether group.

### Morphology of the XNBR films

Figure 3 shows the morphologies of the unfilled XNBR film and XNBR filled with 15-phr fillers at 2000 $\times$  magnification. From the micrograph shown in Figure 3(b), the white portions observed were assumed to be from the highly branched aggregates of the silica filler particles, which showed a homogeneous distribution of silica filler particles within the XNBR latex. This homogeneous distribution increased the interfacial bonding between the filler and the matrix polymer and, thus, increased the mechanical properties of the XNBR/silica films. The surface energy of the filler influenced the compatibility with the elastomer. Silica is highly polar and does not interact well with a nonpolar elastomer. Because the XNBR latex contained —COOH groups, which are polar groups, this resulted in better interaction between the silica filler and the XNBR latex (matrix).

Figure 3(c) shows that the 15-phr mica filler possessed a different morphology from the silica-filled XNBR. We believe that the dispersions of the mica flakes in the XNBR latex were very poor, as evidenced by many large mica flake aggregates and a large amount of XNBR latex matrix without mica fillers. Microstructural studies by Xavier et al.<sup>6</sup> revealed that the mica concentration influences the mica flake orientation and, thereby, affects the relative skin core zone thicknesses; these, in turn, affect the mechanical performance of the films. From As shown in Figure 3(d), the morphology of the 15-phr



**Figure 4** Effect of the different types of fillers and filler loadings on the tensile strength of the XNBR latex films. [Color figure can be viewed in the online issue, which is available at [wileyonlinelibrary.com](http://wileyonlinelibrary.com).]

CB filler was evenly distributed in the XNBR latex film. This showed that CB could effectively reinforce the XNBR latex film. This result was supported by excellent mechanical properties shown by various tests, as discussed later. The morphology shown in Figure 3(e) showed that the XNBR/CaCO<sub>3</sub> latex film possessed the same morphology as the mica-filled XNBR latex film. We believe that the dispersions of the CaCO<sub>3</sub> particles in the XNBR latex were very poor, as evidenced by the aggregation of the CaCO<sub>3</sub> particles within the XNBR latex. This resulted from different particles sizes of the fillers used; the average filler size for N330 CB was 28–36 nm, that for colloidal silica was 30–100 nm, that for the mica flakes was 15–150 μm, and that for CaCO<sub>3</sub> was greater than 2 μm.

### Tensile properties

The mechanical properties for the XNBR latex films with silica, mica, CB, and CaCO<sub>3</sub> are shown in Figure 4 and Table V. As shown in Figure 4, the films with silica, mica, and CB showed increases in the tensile strength compared to the unfilled XNBR latex. CaCO<sub>3</sub> did not show the reinforcing effect on the XNBR latex films because of the nature of this filler, which is normally added to latex compounds to reduce the cost. Table V shows the effect of the fillers on Modulus at 100% elongation (M100) and Modulus at 300% elongation (M300). M100 and M300 showed an increase in the modulus for all fillers, except mica, which showed a decrease.

The increases in the tensile strength and modulus of the XNBR latex films with different types of fillers could be explained on the basis of the morphological structure of the ionic elastomer or ionomer. The incorporation of ZnO in XNBR produced a new type of polymer called an ionic elastomer; in general an *ionomer* is a polymer in which carboxyl groups neutralized by ZnO cause the incorporation of ionic

crosslinking. The high tensile strength value resulted from the incorporation of ions and their aggregations.

The tensile strength properties shown in Figure 4 illustrate that the tensile strengths of the silica-filled XNBR latex films increased at the beginning and reached an optimum value when the silica filler content was at 15 phr; then, they decreased with further increases in the silica loading. The initial increase in the tensile strength with an increase in silica loading could be explained by the reinforcing effect of the fine silica filler and also by the increase in the crosslinking density of the films. The negative effect on the tensile strength observed at high silica loadings could be explained by the agglomeration of the silica filler.

Silica has a high polar component and has a higher tendency to form a stronger filler–filler network and a weak filler–rubber network.<sup>10</sup> Silica filler also possesses many hydroxyl groups on its surface; this results from the strong intermolecular hydrogen bonds between the hydroxyl groups on the surface of silica, which can form tight aggregates. At a high silica loading, fewer rubber matrices are available to hold the silica particles together; this results in poorer tensile strength. In the case of mica filler, an increase in the filler loading also increased the tensile strength up to 15 phr, whereas further addition of the filler reduced the tensile strength. This result suggests that poor dispersions of the mica filler in the elastomeric matrix contributed to the trend observed. The XNBR film with 20-phr mica filler presented lower stability compared to those with 10- and 15-phr mica filler.

The tensile strength of the XNBR/CB films showed that the reinforcing effect of CB in the XNBR latex films was superior compared to those of the other fillers. The increase in the tensile strength upon the addition of CB continued over the entire range studied. Bandyopadhyay et al.<sup>16</sup> observed a high activity of CB and its oxidized surface, which increased with increasing degree of crosslinking of the fillers–elastomers. They believed this was due to the formation of chemical and physical bonds (weak hydrogen bonds and van der Waals forces) between the carboxylic groups of the rubber and reactive groups on the filler surfaces.

On the other hand, the result shown in Figure 4 indicates that the unfilled XNBR latex film possessed a relatively high tensile strength without the addition of CaCO<sub>3</sub> filler. However, with increasing CaCO<sub>3</sub> loading, the tensile strength of the XNBR/CaCO<sub>3</sub> films increased accordingly. The results obtained were in agreement with the finding by Mandal and Tripathy.<sup>17</sup> They observed increases in the modulus and tear strength of ZnO-cured XNBR with decreasing tensile strength with increased in

**TABLE V**  
Tensile Modulus Values (M100 and M300) for the Unfilled and Filled XNBR Latex Films

Filler content	M100	M300
Control	1.342	2.609
10-phr silica	1.949	3.020
15-phr silica	2.141	3.147
20-phr silica	2.481	3.204
10-phr mica	1.778	2.841
15-phr mica	1.271	2.372
20-phr mica	1.570	2.497
10-phr CB	2.215	5.711
15-phr CB	2.025	3.579
20-phr CB	1.945	3.476
10-phr CaCO <sub>3</sub>	1.528	2.547
15-phr CaCO <sub>3</sub>	1.663	2.635
20-phr CaCO <sub>3</sub>	1.221	2.332

CaCO<sub>3</sub> loading. As shown in Figure 4, the most optimum compositions of filler loading were 15 phr for silica and 10 phr for mica. Further increase in the filler loading showed a decreased in the tensile strength properties. For both CaCO<sub>3</sub> and CB, the maximum tensile strength was obtained at 30 phr.

Generally, when latex films are reinforced with fillers, the particle diameter of the reinforcing agent is the main factor in its reinforcing ability. Smaller particle fillers will have a greater specific surface area. The surface effect tends to be stronger, and this will, in turn, increase the contact area between the filler and the rubber particles and ensure the formation of physical entanglement.<sup>16</sup> At the same time, the capability to inhibit the movement of macromolecules and the carrying efficiency increases, which results in a good reinforcing effect. When the amount of the reinforcing filler exceed a critical value, however, the contact of the rubber particles with the reinforcing particles tend to be saturated. If the amount of reinforcing fillers continues to increase, the aggregates become larger, and the distance between the rubber particles increases; this breaks down the monolithic construction of the material and contributes to poor reinforcement capabilities.<sup>5</sup>

Figure 5 shows the effects of the filler loadings of different types of filler on the elongation at the break properties of the XNBR latex films. For XNBR latex incorporated with CB filler, the percentage of elongation decreased drastically with the addition of filler; this indicated interference by the filler to the mobility or deformability of the matrix. This interference was created through physical interaction and, thereby, rendered the polymer matrix immobile by the imposition of mechanical restraints.

At a higher filler loading, the interstitial volume was occupied by the smaller particle size filler, and there may not have been enough matrices available to contribute to the percentage of elongation. In this

context, agglomerates or flocculated particles at a higher filler loading provided a higher modulus (Table V) because the portion of the matrix that was isolated in the agglomerates was less free to react to stress and strain than the continuous phase at values below the maximum packing fraction.<sup>5</sup> The elongations at break tended to increase initially when the XNBR latex was incorporated with the silica and mica fillers. When the amount of silica was increased to 15 phr, the comprehensive efficiency was optimum; when it was greater than 15 phr, the reinforcing effect decreased. For the mica filler, the efficiency was optimum when 10 phr filler was incorporated and decreased with the further addition of fillers.

### Tear properties

As shown in Figure 6, with the addition of various types of fillers in the XNBR latex films, the value of tear strength increased. This effect was more pronounced in the case of the CB-filled XNBR latex films. In the range of fillers studied, critical filler loadings were observed. These were 15 phr for silica- and mica-filled XNBR latex films, whereas for films filled with CB and CaCO<sub>3</sub>, the tear strength did not achieve the limit of saturation. The tear strength continued to increase with the addition of filler.

Generally, the tear strength increased in all of the XNBR latex films with the addition of fillers because of the increase in rubber–filler interaction in the bulk of the polymer and also because of cluster–filler interaction. These clusters were formed by the reaction between –COOH and ZnO.<sup>18</sup> The cluster model, in which there is restricted mobility of the polymer chains in the vicinity of the ionic multiplets, gives rise to the hard phase. The association of the multiplets formed clusters. In the presence of the

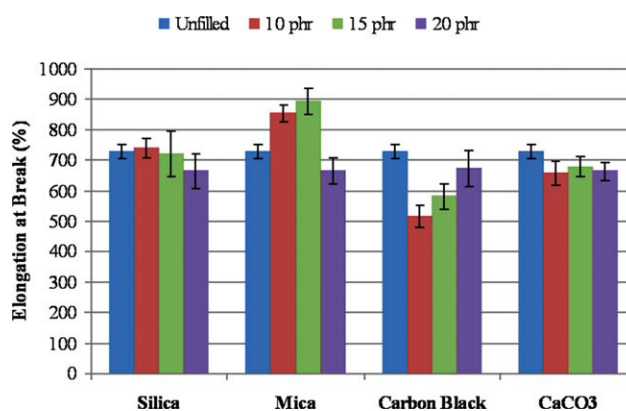


**Figure 5** Effect of the different types of fillers and filler loadings on the elongation at break of the XNBR latex films. [Color figure can be viewed in the online issue, which is available at [wileyonlinelibrary.com](http://wileyonlinelibrary.com).]

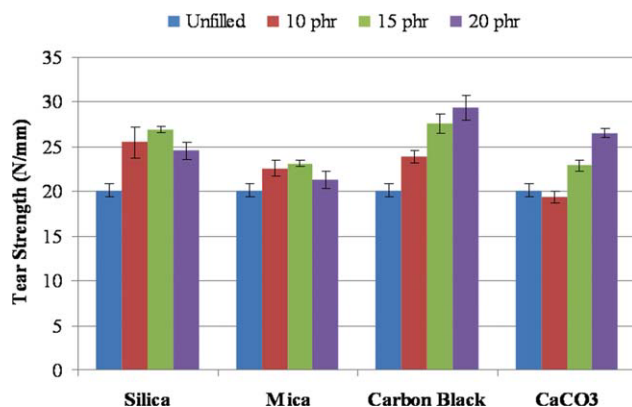


**Figure 6** Effect of the different types of fillers and filler loadings on the tear strength of the XNBR latex films. [Color figure can be viewed in the online issue, which is available at [wileyonlinelibrary.com](http://wileyonlinelibrary.com).]

reinforcing filler, ionic aggregation is favored, and this increases the elastic modulus significantly; thus, the tear strength increases because of rubber–filler interaction in the bulk of the polymer and because of cluster–filler interaction.<sup>19</sup>

### Crosslinking density measurements

Figure 7 shows the effect of the filler loadings of different types of fillers on the crosslinking density of the XNBR latex films. According to numerous studies, silica and mica are widely known to have strong filler–filler interaction due to the silanol groups (Si–OH) that cover the surfaces of silica and mica. They have a very strong tendency to form hydrogen bonding between them; this results in a strong agglomeration between silica and mica entities.<sup>7,20–25</sup> Therefore, an increase in silica loading should lead to an increase in silica–silica and mica–mica interac-

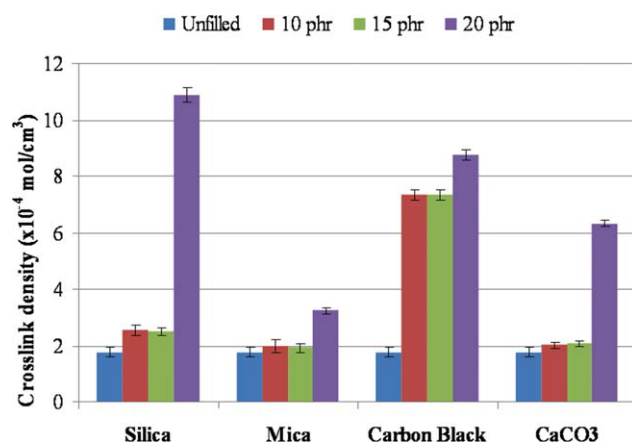


**Figure 7** Effect of the different types of fillers and filler loadings on the crosslink density of the XNBR latex films. [Color figure can be viewed in the online issue, which is available at [wileyonlinelibrary.com](http://wileyonlinelibrary.com).]

tion and, hence, to a decrease in the filler–rubber interaction.

The crosslinking density of the carbon-black-filled XNBR latex films increased with increasing filler loading. Changes in the crosslinking density of the XNBR latex films with increasing CB loading could be explained as the consequence of the existing pressure involved between the XNBR elastomer network and the solvent, which acted to expand or shrink the elastomer network. The crosslinking density increased drastically with an increase in filler loading; this resulted in an increase in the network elasticity contributions. These crosslinks restricted the extensibility of the elastomer chains induced by swelling and made it more difficult for the solvent to diffuse between the gaps of the elastomer molecules. This decreased the swelling percentage and, thus, countered any tendency for dissolution. Therefore, the swelling decreased with increasing networks.

### CONCLUSIONS

The following conclusions were drawn from this study:

1. The tensile properties, crosslinking density, and tear strength of the XNBR films were altered with filler addition as a result of the filler–rubber interactions. Furnace ashing and FTIR analysis proved that chemical bonding existed between the fillers and the XNBR latex films.
2. SEM at high magnification (2000 $\times$ ) showed that the XNBR latex films incorporated with silica and mica fillers enclosed the filler agglomeration, which contributed to the decrease in mechanical properties at higher filler loadings.
3. The addition of fillers such as silica, mica, and CB improved the mechanical properties of the XNBR latex, which signified the reinforcing effect of silica, mica, and CB as fillers. Silica and mica fillers showed the reinforcing effect at lower filler loadings, whereas CB showed the reinforcing effect at a higher filler loading.
4. CB gave the best reinforcing effects for the XNBR latex films because of better filler–rubber interaction, as confirmed by the higher crosslinking density and strength properties.

### References

1. Mayo Foundation for Medical Education and Research (MFMER). <http://www.mayoclinic.com/health/latex-allergy/DS00621/DSECTION=causes> (accessed on 2 August 2010).
2. Zhang, Y.; Ge, S.; Tang, B.; Koga, T.; Rafailovich, M. H.; Sokolov, J. C.; Peiffer, D. G.; Li, Z.; Dias, A. J.; McElrath, K. O.; Lin,



- M. Y.; Satija, S. K.; Urquhart, S. G.; Ade, H.; Nguyen, D. *Macromolecules* 2001, 34, 7056.
3. Castro, D. F.; Suarez, J. C. M.; Nunes, R. C. R.; Visconte, L. L. Y. *J Appl Polym Sci* 2003, 90, 2156.
  4. Chronska, K.; Przepiorkowska, A. *J Hazard Mater* 2008, 151, 348.
  5. Kashani, M. R.; Padovan, J. *Plast Rubber Compos* 2007, 36, 47.
  6. Xavier, S. F.; Schultz, J. M.; Friedrich, K. *J Mater Sci* 1990, 25, 2421.
  7. Blackley, D. C. *Polymer Latices*, 2nd ed.; Springer: Chapman and Hall, London, UK, 1997; Vol. 2.
  8. Mecadi. Carboxylated-Nitrile-Butadiene-Rubber (XNBR). [http://www.functionalpolymer.com/en/literature\\_tools/encyclopedia/categorial/Copolymer/Carboxylated-Nitrile-Butadiene-Rubber\\_XNBR](http://www.functionalpolymer.com/en/literature_tools/encyclopedia/categorial/Copolymer/Carboxylated-Nitrile-Butadiene-Rubber_XNBR) (accessed May 2010).
  9. Flory, P. J.; Rehner, J., Jr. *Chem Phys* 1943, 1, 521.
  10. Kohls, D. J.; Baucage, G. *Curr Opin Solid State Mater Sci* 2002, 6, 183.
  11. Mandal, U. K. *Polym Int* 2000, 49, 1653.
  12. Chakraborty, S.; Bandyopadhyay, S.; Ameta, R.; Mukhopadhyay, R.; Deuri, A. S. *Polym Test* 2007, 26, 38.
  13. Gunasekaran, S.; Natarajan, R. K.; Kala, A. *Spectrochim Acta A* 2007, 68, 323.
  14. Tulyapitak, T. Ph.D. thesis, University of Akron, 2006, p 204.
  15. Jing, S. Y. *J Korean Phys Soc* 2002, 41, 769.
  16. Bandyopadhyay, S.; De, P. P.; Tripathy, D. K.; De, S. K. *Polymer* 1996, 32, 353.
  17. Mandal, U. K.; Tripathy, D. K. *Kautsch Gummi Kunstst* 1997, 50, 630.
  18. Ibarra, L.; Marcos-Fernandez, A.; Alzorriz, M. *Polymer* 2002, 43, 1649.
  19. Mandal, U. K.; Aggarwal, S. *Polym Test* 2001, 20, 305.
  20. Suzuki, N.; Ito, M.; Yatsuyanagi, F. *Polymer* 2005, 46, 193.
  21. Zhu, A.; Cai, A.; Yu, Z.; Zhou, W. *J Colloid Interface Sci* 2008, 322, 51.
  22. Das, A.; De, D.; Naskar, N.; Debnath, S. C. *J Appl Polym Sci* 2006, 99, 1132.
  23. Shin, C. H.; Kim, D. S. *Polym Adv Technol* 2008, 19, 1062.
  24. Zhang, W.; Leonov, A. I. *J Appl Polym Sci* 2001, 81, 2517.
  25. Furtado, C. R. G.; Leblanc, J. L.; Nunes, R. C. R. *Eur Polym J* 2000, 36, 1717.